LIMNOLOGY
and
OCEANOGRAPHY

ASLO

Limnol. Oceanogr. 00, 2016, 00–00

doi: 10.1002/lno.10329

Differential N_2O dynamics in two oxygen-deficient lake basins revealed by stable isotope and isotopomer distributions

Christine B. Wenk,[a*1] Caitlin H. Frame,[1] Keisuke Koba,[2,3] Karen L. Casciotti,[4] Mauro Veronesi,[5] Helge Niemann,[1] Carsten J. Schubert,[6] Naohiro Yoshida,[7,8,9] Sakae Toyoda,[8] Akiko Makabe,[2,8] Jakob Zopfi,[1] Moritz F. Lehmann[1]

[1]Department of Environmental Sciences, University of Basel, Basel, Switzerland
[2]Faculty of Agriculture, Tokyo University of Agriculture and Technology Fuchu, Tokyo, Japan
[3]Center for Ecological Research, Kyoto University, Shiga, Japan
[4]Department of Earth System Science, Stanford University, Stanford, California
[5]Institute of Earth Sciences, University of Applied Sciences of Southern Switzerland, Canobbio-Lugano, Switzerland
[6]Department of Surface Waters-Research and Management, Swiss Federal Institute of Aquatic Science and Technology (EAWAG), Kastanienbaum, Switzerland
[7]Department of Environmental Chemistry and Engineering, Tokyo Institute of Technology, Tokyo, Japan
[8]Department of Environmental Science and Technology, Tokyo Institute of Technology, Tokyo, Japan
[9]Earth-Life Science Institute, Tokyo Institute of Technology, Tokyo, Japan

Abstract

Lakes are a nitrous oxide (N_2O) source to the atmosphere, but the biogeochemical controls and microbial pathways of N_2O production are not well understood. To trace microbial N_2O production (denitrification, nitrifier denitrification, and nitrification) and consumption (denitrification) in two basins of Lake Lugano, we measured the concentrations and N and O isotope compositions of N_2O, as well as the intramolecular ^{15}N distribution, i.e., site preference (SP). Our results revealed differential N_2O dynamics in the two lake basins, with N_2O concentrations between 12 nmol L^{-1} and >900 nmol L^{-1} in the holomictic South Basin, and significantly lower concentrations in the meromictic North Basin (<13 nmol L^{-1}). In the South Basin, the isotope signatures reflected a complex combination of N_2O production by nitrifying bacteria through hydroxylamine (NH_2OH) oxidation, N_2O production through incomplete denitrification, and N_2O reduction to N_2, all occurring in close vicinity within the redox transition zone (RTZ). In the North Basin, in contrast, the N_2O isotopomer signatures suggested that nitrifier denitrification was the main N_2O source. The pronounced decrease in N_2O concentrations to undetectable levels within the RTZ, in tandem with an increase in $\delta^{15}N\text{-}N_2O$, $\delta^{18}O\text{-}N_2O$, and SP indicated quantitative N_2O consumption by microbial denitrification. In the northern basin this was primarily sulfide-dependent. The apparent N and O isotope enrichment factors associated with net N_2O consumption were $^{15}\varepsilon \approx 3.2‰$ and $^{18}\varepsilon \approx 8.6‰$, respectively. The according ^{18}O to ^{15}N enrichment ratio ($^{18}\varepsilon$: $^{15}\varepsilon \approx 2.5$) is consistent with previous reports for microbial N_2O reduction, underscoring its robust nature across environments.

Nitrous oxide (N_2O) is a potent greenhouse gas and a major ozone-depleting substance in the stratosphere (Wang et al. 1976; Rasmussen and Khalil 1986; Ravishankara et al. 2009). The recent increase in atmospheric N_2O is mainly due to human alteration of the nitrogen (N) cycle, in particular the increased use of synthetic N-based fertilizers (Mosier et al. 1998). Regional watershed N-balance studies have revealed that most of the anthropogenic N input is transferred to gaseous forms before reaching the ocean, making terrestrial ecosystems important sites for fixed N loss, but also for potential N_2O production (Howarth et al. 1996; Alexander et al. 2000; Snider et al. 2015). Terrestrial N-load mitigation can partly be attributed to microbial processes in redox transition zones (RTZs) of lakes. The reactions that affect net N_2O production include: Denitrification, nitrifier denitrification, and nitrification. Denitrification is the stepwise dissimilatory reduction of nitrate (NO_3^-) to nitrite

*Correspondence: christine.wenk@weizmann.ac.il

[a]Present address: Department of Earth and Planetary Sciences, Weizmann Institute of Science, Rehovot, Israel

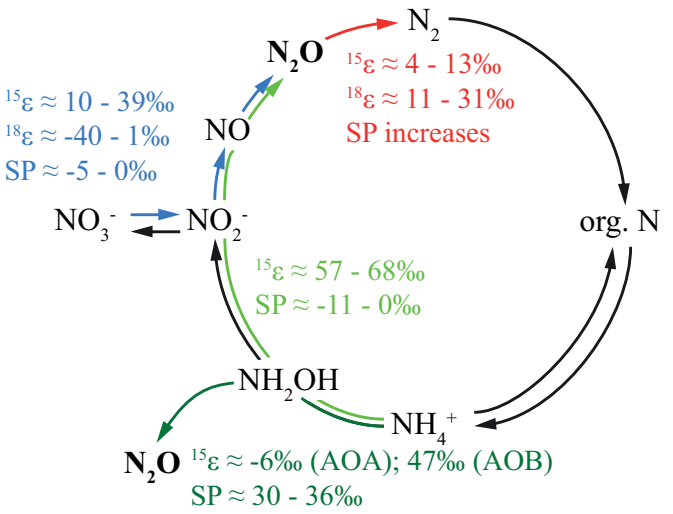

Fig. 1. Schematic illustration of N_2O forming and consuming processes in the microbial N cycle. The N (and O) isotope effects and site preferences (SP) of produced N_2O are given for denitrification (blue), nitrification (dark green), and nitrifier denitrification (light green), as well as for N_2O consumption by denitrification (red). $^{15}\varepsilon \approx \delta^{15}N_{substrate} - \delta^{15}N_{product}$; $^{18}\varepsilon \approx \delta^{18}O_{substrate} - \delta^{18}O_{product}$; AOA = ammonia oxidizing archaea; AOB = ammonia oxidizing bacteria.

(NO_2^-), nitric oxide (NO), N_2O, and dinitrogen gas (N_2), and is the only known pathway for N_2O consumption (Fig. 1). If incomplete, both organotrophic (i.e., oxidation of organic molecules to obtain energy) and lithotrophic (i.e., oxidation of inorganic molecules to obtain energy) denitrification can also lead to the accumulation of N_2O (Baumann et al. 1997; Rakshit et al. 2008). Nitrifier denitrification, the reduction of NO_2^- to N_2O by nitrifying bacteria (and possibly archaea) under hypoxic conditions, with O_2 concentrations of a few μmol L^{-1}, is another potential N_2O source (Fig. 1) (Poth and Focht 1985; Wrage et al. 2001; Treusch et al. 2005). Nitrification, the aerobic oxidation of ammonium (NH_4^+) to NO_2^- and NO_3^- can lead to N_2O production through chemical decomposition of the intermediate hydroxylamine (NH_2OH) (Hooper and Terry 1979). The exact mechanism of this N_2O formation from NH_2OH is unclear. A possible intermediate is nitroxyl (HNO) (Bonner and Hughes 1988), which then reacts to hyponitrous acid ($H_2N_2O_2$) (Toyoda et al. 2002; Schmidt et al. 2004) and eventually dehydrates to N_2O (Fehling and Friedrichs 2011). Other potential abiotic N_2O production mechanisms invoke the reaction of NO_2^- with NH_2OH (Bonner et al. 1983; Heil et al. 2014), or the reduction of NO_2^- with Fe^{2+} (Wullstein and Gilmour 1966; Jones et al. 2015). While these abiotic reactions have been confirmed in incubation experiments with substrate concentrations in the mmol L^{-1} range, it is not clear as to how important they are in natural environments, where concentrations are much lower (Zhu et al. 2013).

A powerful tool to study N_2O production and consumption processes is the measurement of the stable N and O isotope composition of N_2O. The value of such measurements is based on the fact that most N_2O sources display characteristic isotope signatures, which can be used to diagnose the relative importance of different N_2O producing reactions (e.g., Wunderlin et al. 2013). For example, it has been shown that organotrophic denitrification to N_2O proceeds with a relatively large isotope fractionation between NO_3^- and N_2O, with $^{15}\varepsilon_{NO_3^-\rightarrow NO_2^-}$ (= $\delta^{15}N_{NO_3^-}$ – bulk $\delta^{15}N_{N_2O}$) ranging between 10‰ and 39‰ and $^{18}\varepsilon_{NO_3^-\rightarrow N_2O}$ (=$\delta^{18}O_{NO_3^-}$ – $\delta^{18}O_{N_2O}$) between −40‰ and 1‰ (Fig. 1, Table 1) (Barford et al. 1999; Casciotti et al. 2002; Toyoda et al. 2005; Sutka et al. 2006). Large N isotope fractionation between NH_4^+ and N_2O is also observed for nitrifier denitrification ($^{15}\varepsilon_{NH_4^+\rightarrow N_2O} \approx$ 57‰–68‰) (Yoshida 1988; Frame and Casciotti 2010) and for bacterial nitrification ($^{15}\varepsilon_{NH_4^+\rightarrow N_2O} \approx$ 47‰) (Sutka et al. 2006). In contrast, ammonia oxidizing archaea (AOA) seem to produce N_2O that is enriched in ^{15}N relative to the source NH_4^+ ($^{15}\varepsilon_{NH_4^+\rightarrow N_2O} \approx$ −6‰) (Santoro et al. 2011; Stieglmeier et al. 2014). While bacterial N_2O production yields N_2O that is relatively depleted in both ^{15}N and ^{18}O relative to the respective substrate, N_2O reduction leaves the residual N_2O enriched in the heavy isotopes. The isotope effects associated with N_2O reduction are $^{15}\varepsilon_{N_2O\rightarrow N_2} \approx$ 4‰–13‰ and $^{18}\varepsilon_{N_2O\rightarrow N_2} \approx$ 11‰–31‰, respectively (Fig. 1) (Barford et al. 1999; Ostrom et al. 2007; Yamagishi et al. 2007).

Similar to the bulk stable isotope composition of N_2O, the quantification of N_2O isotopomers, i.e., the determination of the intramolecular distribution of ^{15}N within N_2O can provide valuable information on N_2O consuming and producing processes. The ^{15}N-site preference (SP), which quantifies the partitioning of ^{15}N between the central (α) and terminal (β) positions within the asymmetric N_2O molecule, is defined as $SP = \delta^{15}N^{\alpha} - \delta^{15}N^{\beta}$ (Toyoda and Yoshida 1999) and typically ranges from 30‰ to 36‰ for both bacterial and archaeal nitrification (Sutka et al. 2003, 2004, 2006; Frame and Casciotti 2010; Santoro et al. 2011), probably due to the production of N_2O from the nitrification intermediate NH_2OH (Fehling and Friedrichs 2011; Heil et al. 2014; Yamazaki et al. 2014). Conversely, N_2O production through incomplete denitrification or nitrifier denitrification is catalyzed by enzymatic reactions, yielding SP values of −5‰ to 0 and −11‰ to 0, respectively (Sutka et al. 2003, 2004, 2006; Toyoda et al. 2005; Frame and Casciotti 2010). Fractionation during N_2O reduction to N_2 increases the SP of the residual N_2O (Ostrom et al. 2007; Yamagishi et al. 2007). This is most probably due to the preferential N-O bond breakage of N_2O molecules with ^{14}N in the α-position, leaving the residual N_2O enriched in ^{15}N at the α-position. In contrast to the bulk N and O isotope composition of N_2O, the SP is thought to be independent of the isotopic composition of the precursor substrate. SP has been used to trace metabolic N_2O production and consumption processes in environments with

Table 1. Reported values for N and O isotope effects associated with N_2O production and consumption, and ^{15}N site preference values for produced N_2O.

Reaction	$^{15}\varepsilon$ [‰]*	$^{18}\varepsilon$ [‰]**	SP [‰]	Organism	Reference
Denitrification:					
$NO_3^- \rightarrow NO_2^- \rightarrow NO \rightarrow N_2O$					
	13		−1	*P. chlororaphis*	Sutka et al. (2006)
	37		−1	*P aureofaciens*	Sutka et al. (2006)
		−40		*P. aureofaciens*	Casciotti et al. (2002)
	10 to 22	−23 to −4	−5	*P. denitrificans*	Toyoda et al. (2005)
	29			*P. denitrificans*	Barford et al. (1999)
	17 to 39	−32 to 1	23	*P. fluorescens*	Toyoda et al. (2005)
Nitrifier denitrification:					
$NH_4^+ \rightarrow NH_2OH \rightarrow NO_2^- \rightarrow NO \rightarrow N_2O$					
	60 to 68			*N. europaea*	Yoshida (1988)
	57		−11	*N. marina*	Frame and Casciotti (2010)
$NO_2^- \rightarrow NO \rightarrow N_2O$					
	35		−1	*N. europaea*	Sutka et al. (2003, 2004)
	24		0	*N. multiformis*	Sutka et al. (2006)
Nitrification:					
$NH_4^+ \rightarrow NH_2OH \rightarrow N_2O$					
			36	*N. marina*	Frame and Casciotti (2010)
	47		31	*N. europaea*	Sutka et al. (2006)
	−6		30	*Archaeon CN25*	Santoro et al. (2011)
$NH_2OH \rightarrow N_2O$					
	−2		34	*N. europaea*	Sutka et al. (2006)
	−2		33	*N. multiformis*	Sutka et al. (2006)
	−3		31	*M. capsulatus*	Sutka et al. (2003, 2004)
	−6		36	*M. trichosporium*	Sutka et al. (2006)
			30	Inorganic oxidation	Toyoda et al. (2005)
Denitrification:					
$N_2O \rightarrow N_2$					
	13			*P. denitrificans*	Barford et al. (1999)
	4	11		*P. stutzeri*	Ostrom et al. (2007)
	7	15		*P. denitrificans*	Ostrom et al. (2007)
	12	31		Denitrification in OMZ	Yamagishi et al. (2007)

*$^{15}\varepsilon \approx \delta^{15}N_{substrate} - \delta^{15}N_{product}$; ** $^{18}\varepsilon \approx \delta^{18}O_{substrate} - \delta^{18}O_{product}$.

mixed microbial communities, such as wastewater treatment plants (Wunderlin et al. 2013), soils (Snider et al. 2009), groundwater (Koba et al. 2009), the open ocean (Popp et al. 2002; Westley et al. 2006; Yamagishi et al. 2007), and lakes (Sasaki et al. 2011).

Here, we use N_2O stable isotope and isotopomer measurements to gain insight into the N_2O dynamics in two biogeochemically distinct basins of Lake Lugano in southern Switzerland. The southern basin is holomictic, with strong density stratification and bottom water anoxia during summer and fall, and a water column overturn usually in January/February (Lehmann et al. 2004; Wenk et al. 2014b). The dominant fixed N removal process appears to be organotrophic denitrification within the sediments (Wenk et al. 2014b). In contrast, the deeper northern basin is generally stratified throughout the year, although exceptional mixing of the complete water column has occurred during the extremely cold and windy winters of 2005 and 2006 (Holzner et al. 2009; Lehmann et al. 2015). Sulfur-driven denitrification within the water column seems to be the main sink for fixed N, but anaerobic ammonium oxidation (anammox) contributes up to 30% of total N_2 production (Wenk et al. 2013). In this study, we present N_2O concentration measurements, as well as stable isotope and isotopomer distributions of N_2O in the water column (1) to assess the spatio-temporal variability of N_2O accumulation in the two basins, (2) to identify the dominant modes of N_2O production, and (3) to compare the N_2O dynamics between the two basins with

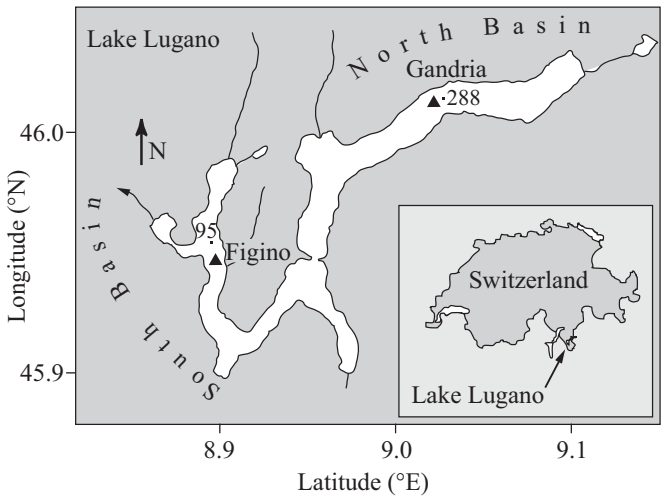

Fig. 2. Location and map of Lake Lugano. The sampling stations are marked by black triangles and are located close to the point of maximum water depth (288 m in the North Basin, and 95 m in the South Basin). Map adapted from Barbieri and Polli (1992).

respect to the different environmental conditions, i.e., the different redox and mixing regimes.

Methods

Study site and sampling

Lake Lugano is located on the southern slopes of the Alps at 271 m above sea level (Fig. 2). A natural dam separates the lake into two main basins. The holomictic southern basin is 95 m deep. This basin is completely ventilated and oxic between February and May. In spring, increased organic matter (OM) mineralization leads to a layer of anoxic bottom water, which expands into the water column during summer and fall, reaching a maximum thickness of about 20 m (Lehmann et al. 2004; Wenk et al. 2014b). The northern basin has a maximum water depth of 288 m and has only mixed twice completely in the last 55 years, during the exceptionally cold and windy winters of 2005 and 2006 (Holzner et al. 2009; Lehmann et al. 2015). Today, the basin is stratified, with a quasi-permanent redox-transition zone and chemocline at 125 m (Wenk et al. 2013; Blees et al. 2014a,b). Samples were collected from both basins at sites west of the village of Figino (45.95°N, 8.90°E) and south of the village of Gandria (46.01°N, 9.02°E), respectively (Fig. 2). Discrete water depths were sampled during hydrocasting, using 5-L and 10-L Niskin bottles within the framework of sampling campaigns in 2009 (August, October), and 2010 (January, August, and October). Temperature and oxygen (O_2) concentration profiles were measured with a conductivity, temperature, depth (CTD) device (Idronaut Ocean Seven 316Plus, Idronaut), and O_2 concentrations were calibrated against Winkler titration measurements. The detection limit for dissolved [O_2] was 1 μmol L^{-1}.

N_2O and nutrient concentrations

For N_2O concentration analyses, water from the Niskin bottle was directly filled into 500 mL glass bottles and immediately sealed with thick butyl rubber stoppers. A 10 mL headspace was introduced, and 10 mL of aqueous NaOH solution (50% w:v) were added in exchange with sample in order to stop microbial activity. N_2O concentrations were determined as described in Diem et al. (2012). Briefly, 40 mL of sample water were replaced with N_2 and equilibrated over night or in an ultrasonic bath for 30 min. Headspace measurements were made on a gas chromatograph (GC, Agilent 6890N) equipped with a GS-CarbonPLOT column (Agilent) and an Electron Capture Detector (ECD). Dissolved gas N_2O concentrations were calculated according to Weiss and Price (1980). The average standard deviation of replicate analyses was 0.3 nmol L^{-1}. Additionally, N_2O concentrations were determined during stable isotope analysis as described below. All NO_3^- and NH_4^+ concentration data have been published recently in Wenk et al. (2013) (North Basin) and in Wenk et al. (2014b) (South Basin). Briefly, separate aliquots of filtered (0.45 μm) lake water were frozen for subsequent analysis of NO_x (i.e., $NO_2^- + NO_3^-$) and NH_4^+. NO_x and NO_2^- concentrations were determined on a NO_x-Analyzer (Antek Model 745) by reduction to nitric oxide (NO) in an acidic V^{3+} or sodium iodide solution, respectively, followed by chemiluminescence detection of NO (Garside 1982; Braman and Hendrix 1989). [NO_3^-] was calculated from the difference of [NO_x] and [NO_2^-]. NH_4^+ concentrations were measured photometrically using the indophenol method (Koroleff 1976).

N_2O isotope and isotopomer analyses

Water aliquots for N_2O isotope and isotopomer analyses were directly sampled into 160 mL glass bottles. For the August 2009 and August 2010 profiles, the bottles were sealed with butyl rubber stoppers without headspace. To stop microbial activity, 0.5 mL of a $HgCl_2$ solution (5% w:v) were introduced in exchange with sample water. During the October 2010 campaign, the samples were fixed by removing 2 mL of sample water and adding 0.1 mL of a $HgCl_2$ solution (5% w:v) before sealing the vials with butyl rubber stoppers. The samples were stored cooled until analysis. Bulk N_2O isotope and isotopomer analyses of samples from August 2009 and 2010 were conducted at the Tokyo Institute of Technology, Japan, using an online analytical system comprising a 200 mL gas extraction chamber (Koshin Rikagaku Seisakusho, Tokyo, Japan), a stainless-steel gas transfer line, preconcentration traps, chemical traps for removal of H_2O and CO_2, and a gas chromatograph/isotope ratio mass spectrometer (MAT 252; Thermo Fisher Scientific Inc.) (Toyoda et al. 2009). Analyses of October 2010 samples were performed at Woods Hole Oceanographic Institution, as described in

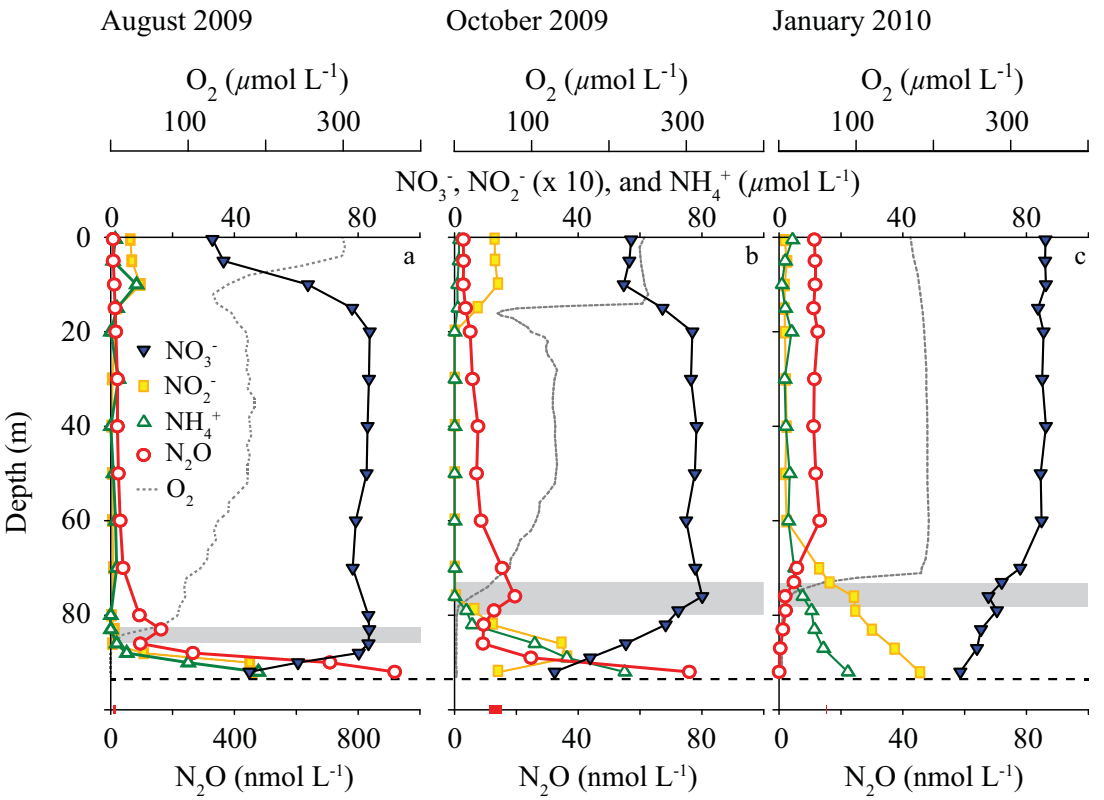

Fig. 3. Water column profiles of dissolved NO_3^-, NO_2^-, NH_4^+, N_2O, and O_2 concentrations from the Lake Lugano South Basin in (a) August 2009, (b) October 2009, and (c) January 2010. The gray bar marks the oxic–anoxic interface, i.e., $[O_2]$ from 50 μmol L^{-1} to <1 μmol L^{-1}. The sediment–water interface is indicated by the dashed black line. The range of N_2O concentrations that would exist if the water was in equilibrium with the atmosphere [calculated according to Weiss and Price (1980)] is marked with a red bar on the $[N_2O]$ scale.

McIlvin and Casciotti (2010). N_2O was purified by passage through chemical traps before cryogenic trapping with liquid nitrogen and release to gas chromatograph/isotope ratio mass spectrometer (Finnigan Delta^{PLUS} XP). Bulk N and O isotope ratios are reported as δ values in ‰ relative to atmospheric N_2 (AIR) and Vienna Standard Mean Ocean Water (VSMOW), respectively, where $\delta = (R_{sample}/R_{standard} - 1) \times 1000$, and $R = {}^{15}N$: ^{14}N or ^{18}O: ^{16}O. The site-specific ^{15}N enrichment values, $\delta^{15}N^{\alpha}$ and $\delta^{15}N^{\beta}$, denote the relative enrichment of ^{15}N in the central (i.e., $^{14}N^{15}N^{16}O$: $^{14}N^{14}N^{16}O$) and in the terminal (i.e., $^{15}N^{14}N^{16}O$: $^{14}N^{14}N^{16}O$) position, and are also reported relative to AIR. Isotopomer calibrations were performed as described by Frame and Casciotti (2010) using three pure N_2O reference gases that were calibrated by Sakae Toyoda. Bulk $\delta^{15}N$-N_2O data are reported on the Tokyo Tech scale (Mohn et al. 2012). The measurement precision was usually better than 0.2‰ for bulk $\delta^{15}N$-N_2O, better than 0.5‰ for $\delta^{18}O$-N_2O, and better than 1.0‰ for SP. Inter-laboratory comparison of isotope measurements were conducted using gas samples, and the offsets between the two laboratories were < 0.1‰, < 1.5‰, and < 4‰ for $\delta^{15}N^{bulk}$, $\delta^{18}O$, and SP, respectively (Mohn et al. 2014). The relatively large inter-laboratory variability in SP was mostly due to the lack of available isotopomer standards at the time of this study (Mohn et al. 2014).

Results

N_2O concentration and isotope composition in the Lake Lugano South Basin

The seasonality of hypolimnetic oxygenation and nutrient cycling in the water column of the Lake Lugano South Basin has been described in detail elsewhere (Lehmann et al. 2004; Blees et al. 2014a, Wenk et al. 2014b). Briefly, winter water column overturn ventilates the hypolimnion, which then remains completely oxygenated between February and May. During the spring and summer months, primary production in the surface water enhances export of organic matter and respiration rates in the hypolimnion, leading to the development of an anoxic layer in the bottom water. Active denitrification within the anoxic water column and the sediment is indicated by decreasing NO_3^- concentrations from mid-water depths toward the sediments. The denitrification and redox transition zones rise into the water column with ongoing water column stratification, and the anoxic, NH_4^+ containing bottom water layer reaches a maximum thickness of about 20 m in late fall and winter. In January, the

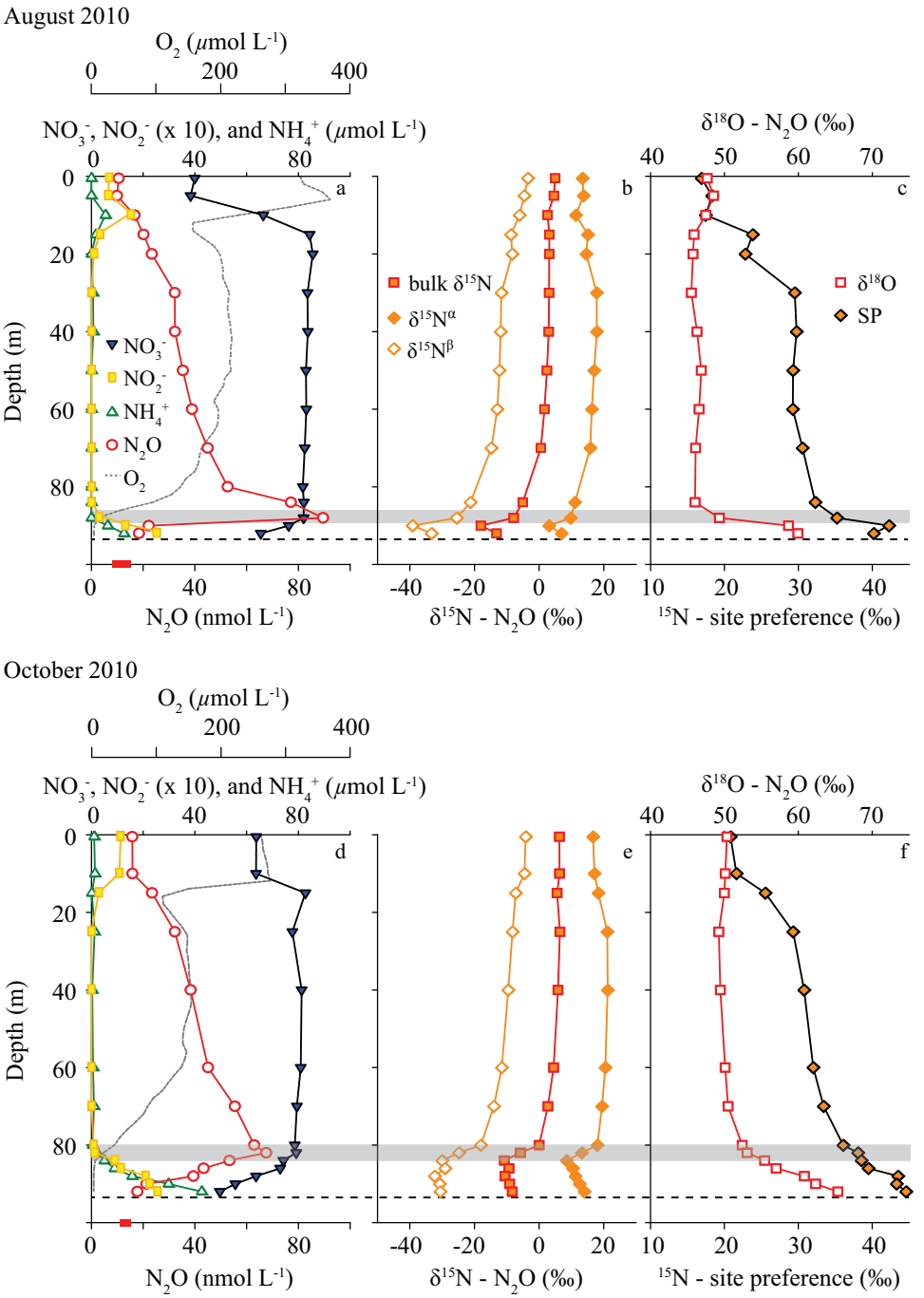

Fig. 4. Dissolved NO_3^-, NO_2^-, NH_4^+, N_2O, and O_2 concentrations (a,d), as well as bulk $\delta^{15}N$–, $\delta^{15}N^{\alpha}$–, and $\delta^{15}N^{\beta}$–N_2O (b,e), and ^{15}N-site preference (SP) and $\delta^{18}O$-N_2O (c,f) in the water column of the Lake Lugano South Basin in August 2010 (a–c) and October 2010 (d–f). The gray bar marks the depth of the oxic–anoxic interface, i.e., $[O_2]$ from 50 μmol L^{-1} to <1 μmol L^{-1}. The sediment–water interface is indicated by the dashed black line. The range of N_2O concentrations that would exist if the water was in equilibrium with the atmosphere [calculated according to Weiss and Price (1980)] is marked with a red bar on the $[N_2O]$ scale.

seasonal cycle starts over again, with the destratification of the water column and the collapse of O_2 and nutrient concentration gradients (Fig. 3).

In August 2009, large amounts of dissolved N_2O accumulated in the anoxic bottom water (Fig. 3a). A maximum concentration of 918 nmol L^{-1} (i.e., ~100 times atmospheric equilibrium level) was measured in the deepest sample 1 m above the sediment–water interface. A second, although weaker N_2O maximum of 163 nmol L^{-1} was detected at the oxic–anoxic interface (i.e., at 83 m depth). The N_2O peak at

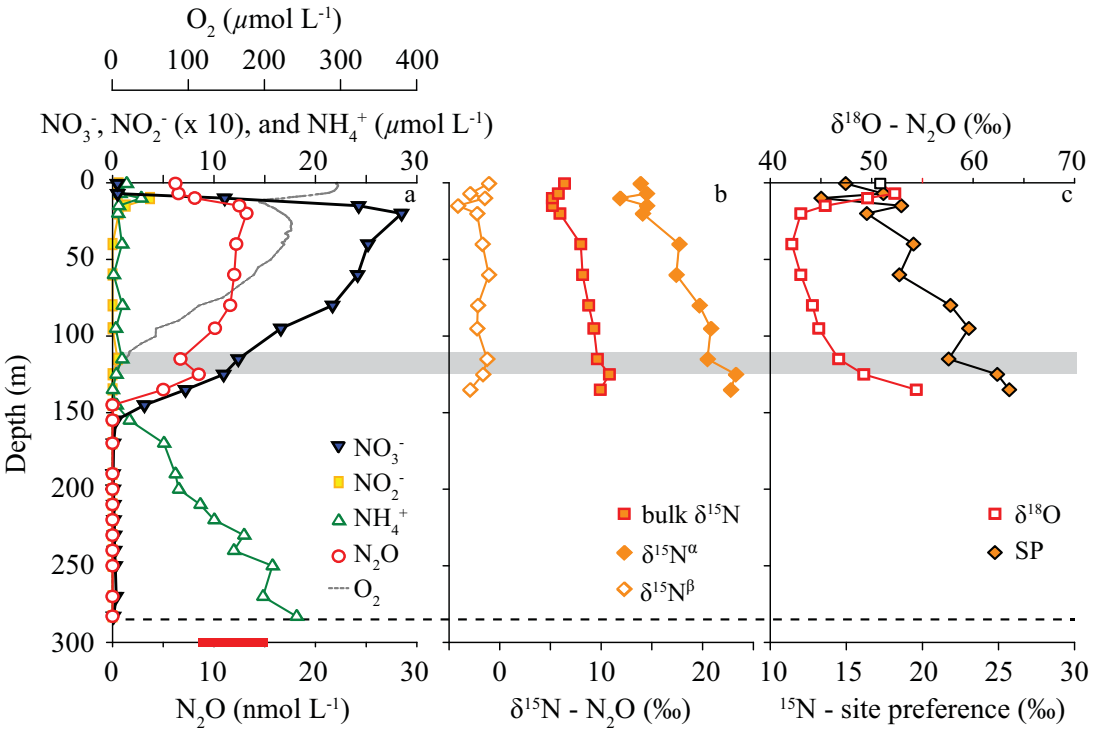

Fig. 5. Water column profiles of (a) NO_3^-, NO_2^-, NH_4^+, N_2O, and O_2 concentrations in the Lake Lugano North Basin in August 2009. Also shown are (b) bulk $\delta^{15}N$–, $\delta^{15}N^{\alpha}$–, $\delta^{15}N^{\beta}$–N_2O, and (c) ^{15}N-site preference (SP), and $\delta^{18}O$-N_2O. The gray bar marks the depth of the oxic–anoxic interface. The sediment–water interface is indicated by the dashed black line. The range of N_2O concentrations that would exist if the water was in equilibrium with the atmosphere [calculated according to Weiss and Price (1980)] is marked with a red bar on the [N_2O] scale.

the oxic–anoxic interface was a feature that occurred during subsequent sampling campaigns, yet at lower concentration levels (see below). In October 2009, maximum N_2O concentrations in the near-bottom water (76 nmol L^{-1}) and peak concentrations at the oxic–anoxic interface (20 nmol L^{-1} at 76 m depth) were significantly lower compared to August 2009 (Fig. 3b). In January 2010, bottom water N_2O accumulation was not observed at all (Fig. 3c). At that time, N_2O concentrations decreased from highest values in the oxic water column (12 nmol L^{-1}) to undetectable levels below the oxic–anoxic interface.

In the subsequent summer season, N_2O dynamics showed a somewhat different pattern (Fig. 4). In August 2010, N_2O concentrations reached a maximum of 90 nmol L^{-1} at the oxic–anoxic interface (88 m depth), similar to the prior sampling campaigns, but, in contrast to 2009, the N_2O concentration dropped to much lower levels (<19 nmol L^{-1}) in the anoxic bottom water below, without an increase toward the sediment–water interface (Fig. 4a). Hence, our data suggest seasonal as well as interannual variations in the timing and extent of maximum N_2O accumulation, and the balance between N_2O production and consumption. In apparent association with the N_2O concentration peak, a bulk $\delta^{15}N$-N_2O minimum of −18.0‰ was observed just below the depth of O_2 disappearance (i.e., at 90 m depth; Fig. 4b). In contrast, the $\delta^{18}O$-N_2O and the ^{15}N-site preference both increased with depth through the oxic–anoxic interface, from 46.0‰ to 58.7‰ and from 32.3‰ to 42.3‰, respectively (Fig. 4c).

A N_2O concentration maximum at the oxic–anoxic interface could still be observed in October 2010, although it had dropped to 68 nmol L^{-1} and shoaled to a depth of 82 m (Fig. 4d). Below this maximum, N_2O concentrations steadily decreased to 18 nmol L^{-1} toward the sediment–water interface. Similar to the previous sampling in August 2010, bulk $\delta^{15}N$-N_2O reached a minimum of −10.8‰ at the depth of O_2 disappearance and just below the N_2O concentration maximum (i.e., at 84 m depth; Fig. 4e). Below this depth, $\delta^{15}N$-N_2O slightly increased to −8.3‰ near the sediment–water interface. SP and $\delta^{18}O$-N_2O both increased with decreasing N_2O concentrations in the anoxic hypolimnion, reaching maximum values of 44.6‰ and 65.3‰, respectively, 1 m above the sediment–water interface (Fig. 4f).

N_2O concentration and isotope composition in the Lake Lugano North Basin

The nitrogen biogeochemistry of the recent years (2009–2011) in this lake basin has been investigated in detail (Wenk et al. 2013, 2014a), and sulfur-driven denitrification was identified as the dominant fixed N removal process in

the RTZ at mid water depth, whereas organotrophic denitrification seemed to be negligible. Denitrification in the RTZ, here defined as the zone between O_2 disappearance and H_2S accumulation, led to a decrease in NO_3^- concentration from ~30 μmol L^{-1} at 20 m depth to zero levels within the RTZ (Fig. 5a). Highest NH_4^+ concentrations were found in the anoxic hypolimnion close to the sediment (~20 μmol L^{-1}). NH_4^+ concentrations decreased toward the RTZ, indicating ammonium oxidation below the oxic–anoxic interface. A stable (both in terms of identity and abundance) community of anammox bacteria coexisted with sulfide-dependent denitrifiers in the water column at the depth of NO_3^- and NH_4^+ disappearance (Wenk et al. 2013). Anammox bacteria were mainly responsible for NH_4^+ consumption, but microaerobic bacterial or archaeal nitrification cannot be fully excluded.

N_2O concentration profiles qualitatively follow the vertical NO_3^- distribution in the water column, with a maximum N_2O concentration of 13 nmol L^{-1} at 20 m depth and a steady decrease to undetectable levels at 145 m depth, i.e., ~15 m below the depth of O_2 disappearance (Fig. 5a). The N_2O concentration decrease was paralleled by a rather subtle increase of the bulk $\delta^{15}N\text{-}N_2O$ from 5.2‰ at 15m depth to 10.8‰ in the RTZ (Fig. 5b). Over the same sample depth interval, we observed a systematic increase of the SP from 16.4‰ to 25.7‰ and of $\delta^{18}O\text{-}N_2O$ from 43.0‰ to 54.4‰, respectively (Fig. 5c).

Discussion

Large amounts of N_2O accumulate in the Lake Lugano South Basin

In August 2009, we observed extreme N_2O oversaturation levels relative to equilibrium with the atmosphere in the anoxic bottom water of the southern basin (Fig. 3a). The maximum N_2O concentration of > 900 nmol L^{-1} was significantly higher than most peak concentrations reported for other lacustrine (Yoh et al. 1983; Sasaki et al. 2011) or marine water column environments (Popp et al. 2002; Westley et al. 2006; Yamagishi et al. 2007). The hydrochemical profiles in August 2009 (Fig. 3a) suggest that N_2O is produced in the deep anoxic water column or the underlying sediments, most likely through incomplete microbial denitrification. From the observed N_2O concentration gradient in the anoxic bottom water, and based on an average vertical turbulent diffusivity (K_z) of 0.49 m^2 d^{-1} (August 2009) (Wenk et al. 2014b), we estimated a sediment-water N_2O flux of 3.1 μmol m^{-2} h^{-1} in August 2009. This flux estimate significantly exceeds N_2O fluxes observed in other lakes, generally ranging between 0.3 μmol m^{-2} h^{-1} and 0.6 μmol m^{-2} h^{-1} (Mengis et al. 1996; Liikanen and Martikainen 2003; McCrackin and Elser 2010). The computed N_2O fluxes were also significantly greater than in October 2009 (0.2 μmol m^{-2} h^{-1} with an average $K_z = 0.34$ m^2 d^{-1}) (Fig. 3b), suggesting strong variability in benthic N_2O production and consumption. In fact, in October 2009, N_2O accumulation in the water column was reduced by an order of magnitude compared to the previous sampling in August 2009 (Fig. 3a,b). At this point, we can only speculate about the mechanisms behind the massive and sporadic N_2O accumulation in the bottom water of the Lake Lugano South Basin. N_2O reduction is thought to be more inertial relative to the other steps involved in enzyme-regulated denitrification (Otte et al. 1996; Baumann et al. 1997), so that a sudden increase in denitrification rates (e.g., stimulated by increased OM inputs following spring algal blooms) could result in a lag phase between the expression of N_2O-reducing enzymes and the actuation of the remaining denitrifying enzymatic machinery. This could possibly lead to a short-term accumulation of N_2O. Moreover, N_2O reductase seems most susceptible to O_2 inhibition (Babbin et al. 2015), so that unstable redox conditions particularly during the initiation phase of water column anoxia would tend to impede the transformation of N_2O to N_2. Another mode of N_2O production in the anoxic bottom water or the underlying sediments could be the abiotic reduction of NO_2^- with Fe^{2+} (chemodenitrification) (Jones et al. 2015). While this process has been shown to occur in soils and in laboratory experiments, we speculate that the NO_2^- (<4 μmol L^{-1}) as well as Fe^{2+} (<0.1 μmol L^{-1}) concentrations are probably too low in the Lake Lugano South Basin (Wenk et al. 2014b). Independent of the dominant controlling mechanisms, net N_2O accumulation is the result of either increased N_2O production rates or reduced N_2O consumption.

In addition to N_2O production in anoxic near-bottom water and/or sediments, the robust, recurrent local N_2O concentration maximum near the oxic–anoxic interface (Fig. 3a,b) indicates a second N_2O source higher up in the water column. While N_2O production through incomplete denitrification cannot be fully excluded at the oxic–anoxic interface, the correspondence between the N_2O concentration peak and the disappearance of both O_2 and NH_4^+ during all sampling campaigns in the southern basin suggests that N_2O production in this zone is linked to nitrifying bacteria or archaea, either through NH_2OH oxidation during nitrification or NO_2^- reduction during nitrifier denitrification.

In addition to the two zones of N_2O production, N_2O consumption within the water column RTZ is evident from the steep N_2O concentration gradient from the sediment toward the oxic–anoxic interface in August and October 2009 (Fig. 3a,b). This prevents much of the N_2O from entering the overlying oxic water column. Interestingly, the apparent N_2O sink right below the oxic–anoxic interface corresponds spatially with the site of NO_2^- accumulation (Fig. 3a,b). This feature has also been observed in oceanic oxygen minimum zones, where NO_2^- accumulation and N_2O consumption co-occur (Ryabenko et al. 2012; Babbin et al. 2015), and may be linked to electron donor-limited (i.e., organic matter, H_2S, or Fe^{2+}) denitrification in this zone. A second N_2O sink is most likely

located within the sediments below the depth of benthic N_2O accumulation, where denitrification consumes NO_3^-, NO_2^-, and N_2O to completion.

In summary, we have identified four zones where potentially different microbial processes affect N_2O dynamics in the Lake Lugano South Basin. The measured N_2O concentrations are the net result of simultaneously occurring N_2O production and consumption processes in close vicinity, so that both rapid production and sluggish or absent consumption may contribute to N_2O accumulation. A comparison between the October 2009 and January 2010 N_2O profiles (Fig. 3b,c), for example, reveals that with ongoing bottom water anoxia through the fall months, N_2O concentrations decreased to undetectable levels in the bottom water, indicating net N_2O consumption. This seasonal trend suggests that N_2O production was greater than N_2O reduction (i.e., complete denitrification) at the beginning of the stratification period, whereas the opposite is true (i.e., negative N_2O balance) during stratified conditions.

In addition to this apparently seasonal trend, we observed significant interannual variability in N_2O dynamics in the Lake Lugano South Basin. In summer 2010, N_2O accumulated again in the water column (Fig. 4a,d), but not to the same extent as observed in August 2009 (Fig. 3a). In both years, the anoxic sediments were a significant N_2O source, as revealed in independent sediment-core flow-through incubations (Freymond et al. 2013). In 2010, however, the high sedimentary N_2O production rates observed by Freymond et al. (2013) in combination with the low N_2O accumulation in the anoxic bottom water suggested efficient N_2O consumption in the RTZ from the beginning of the stratification period. Moreover, in 2010, the highest N_2O concentrations were detected at the oxic–anoxic interface, implying that N_2O production by nitrification or nitrifier denitrification is an important N_2O source. The exact controls on the relative importance of N_2O production vs. consumption remains elusive, yet the fundamentally different N_2O concentration dynamics observed in 2009 vs. 2010 suggest that N_2O accumulation may respond in a very sensitive and possibly unpredictable way to subtle changes in environmental conditions (e.g., redox state, OM flux, availability of Fe^{2+}). In the next section, we analyze the vertical distribution of N_2O isotope ratios in the water column to further identify the various N cycling processes that controlled N_2O accumulation in the deep Lake Lugano South Basin in 2010.

^{15}N site preference measurements indicate that nitrification is the main N_2O-forming process at the oxic–anoxic interface in the South Basin

In August 2010, $\delta^{15}N\text{-}N_2O$ drops to a value as low as $-18.0‰$ at 90 m depth (Fig. 4b). This decrease in $\delta^{15}N\text{-}N_2O$ toward the oxic–anoxic interface in combination with increasing N_2O concentrations is consistent with N_2O production by nitrifying bacteria, but the bulk isotope signature remains ambivalent with regard to the actual mode of N_2O production, i.e., canonical nitrification and N_2O production through NH_2OH oxidation, or nitrifier denitrification and nitrite reduction to N_2O, respectively (Fig. 1). Ammonium in the anoxic bottom water has a $\delta^{15}N$ that varies between $8‰$ and $23‰$, depending on the extent of partial consumption (Wenk et al. 2014b). The $\delta^{15}N$ of nitrite below the oxic–anoxic interface is approximately $-10‰$ (data not shown). Consequently, the drop in $\delta^{15}N\text{-}N_2O$ to $-18.0‰$ as observed at the depth of NH_4^+ and O_2 disappearance in the Lake Lugano South Basin can be explained by either bacterial nitrification or nitrifier denitrification (Fig. 1, Table 1). Archaeal N_2O production is probably negligible, as it would produce N_2O with a relatively high $\delta^{15}N\text{-}N_2O$ (Santoro et al. 2011). However, SP values greater than $32‰$ at the depth of N_2O production during both 2010 sampling campaigns (Fig. 4) suggest a NH_2OH-derived source of N_2O rather than nitrifier denitrification, given that the SP for N_2O from the latter process should be on the order of $-11‰$ to $0‰$ (Fig. 1; Table 1). This finding seems to contradict an earlier study by Lehmann et al. (2003), who argued that nitrification does not play an important role at the oxic–anoxic interface in the Lake Lugano South Basin. The conclusion was based on coupled nitrate N-vs.-O isotope measurements and the absence of a presumably characteristic N-to-O isotope anomaly. However, based on the current understanding of the coupled NO_3^- N and O isotope dynamics, the previously reported NO_3^- isotope data are consistent with nitrification (Wenk et al. 2014a,b). The N_2O isotope data presented here provide evidence that ammonium-oxidizing bacteria are present in the deep Lake Lugano South Basin and sustain N_2O production through NH_2OH oxidation at these depths. Blees et al. (2014a) have recently demonstrated that methane-oxidizing bacteria dominate the bacterial community within the benthic nepheloid layer that forms during summer in the deep South Basin. Enzymatically, some methanotrophs seem capable of nitrification (Stein et al. 2012), and methanotrophic nitrification appears to produce N_2O with an equally high SP as canonical nitrification (Sutka et al. 2006). Although it is not well constrained how widespread this process is in the environment, we speculate that methanotrophic nitrification may be the prime process leading to the observed N_2O concentration peak at the oxic–anoxic interface.

Stable isotope and isotopomer distributions in the anoxic bottom water reflect co-occurring N_2O production through nitrification, incomplete denitrification, and N_2O consumption in close vicinity

In August, and much more pronounced in October 2010, N_2O reduction to N_2 in the water column or in the sediment is indicated by the parallel increase of $\delta^{15}N$, $\delta^{18}O$, and SP toward the sediment and the decrease in N_2O concentration from the oxic–anoxic interface toward the sediment (Fig. 4). An estimate of the N and O isotope enrichment factors

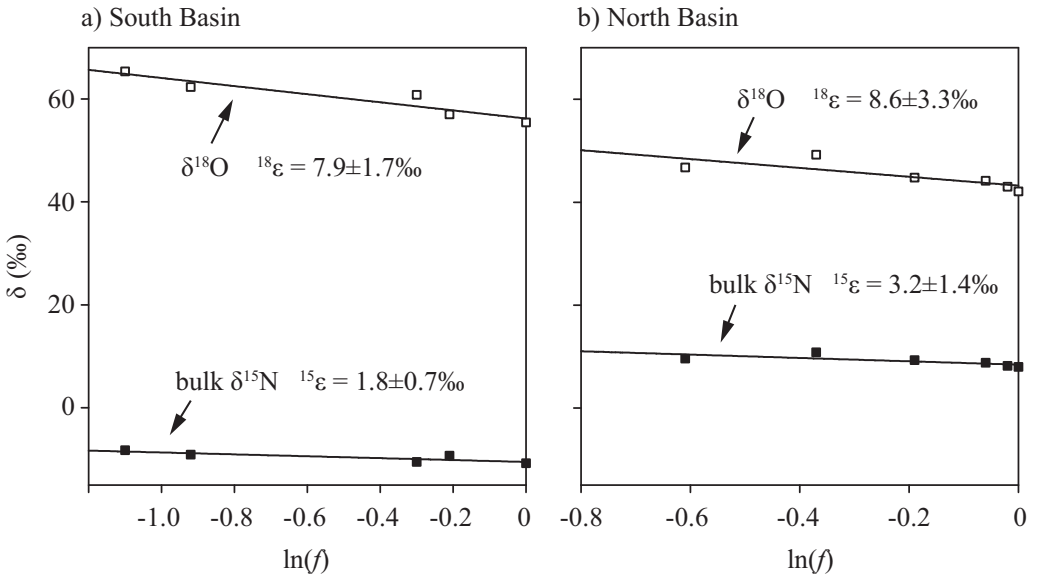

Fig. 6. Rayleigh plots for N_2O consumption in the RTZ of (a) the southern basin in October 2010 and (b) the northern basin in August 2009. The bulk $\delta^{15}N$– and $\delta^{18}O$–N_2O are plotted against ln(*f*), where *f* denotes the remaining N_2O fraction with respect to the concentrations at 84 m (South Basin) and at 40 m (North Basin) water depth. The N and O isotope enrichment factors are approximated by the negative slopes of the linear regression lines (± 1 standard error). For the August 2009 profile, the values from 135 m depth were excluded (see text for details).

associated with this net N_2O consumption was derived from a closed-system (Rayleigh) model (Mariotti et al. 1981). If this model applies to the situation in Lake Lugano, the N_2O isotope composition, $\delta^{15}N$-N_2O or $\delta^{18}O$-N_2O, follows a linear trend with ln(*f*), where *f* is the fraction of the remaining N_2O, relative to the concentration at the oxic–anoxic interface:

$$\delta^{15}N\text{–}N_2O = \delta^{15}N\text{–}N_2O_{source} - {}^{15}\varepsilon \times \ln(f)$$
$$\delta^{18}O\text{–}N_2O = \delta^{18}O\text{–}N_2O_{source} - {}^{18}\varepsilon \times \ln(f)$$

$\delta^{15}N$–N_2O_{source} (or $\delta^{18}O$–N_2O_{source}) is the isotopic composition of the source N_2O at the oxic–anoxic interface and the isotope enrichment factor, ε, is approximated by the slope of the linear regression line. It is important to note that the Rayleigh model is of limited use for the determination of consumption-process-specific ε values in systems that cannot be considered closed, and where N_2O production co-occurs. However, any violation of the closed-system aspect of the Rayleigh approach as evidenced by the clear deviation from expected trends may in turn be used to at least qualitatively diagnose N_2O supply/production within the net N_2O consuming environment. In October 2010, the apparent N and O isotope enrichment factors were ${}^{15}\varepsilon \approx 1.8‰$ and ${}^{18}\varepsilon \approx 7.9‰$, respectively (Fig. 6a). These isotope effects are significantly lower than N and O isotope effects reported for N_2O reduction in natural environments and in culture experiments (Fig. 1; Table 1). The apparent under-expression of the N and O isotope effects in the water column can be explained by sedimentary N_2O consumption or simultaneous N_2O production in the anoxic bottom water or sediments and mixing into the overlying water column. Incomplete denitrification produces N_2O with relatively low $\delta^{15}N$ relative to the substrate, and a SP ≈ 0, potentially shifting the bulk and site-specific ^{15}N isotopic composition in the water column to lower values. Furthermore, N_2O reduction is thought to occur with an ^{18}O to ^{15}N enrichment ratio (i.e., ${}^{18}\varepsilon$: ${}^{15}\varepsilon$) of ~2.5, independent of the degree of isotope fractionation (Yamagishi et al. 2007). In the Lake Lugano South Basin, the ^{18}O to ^{15}N enrichment ratio associated with net N_2O reduction was ~4.4 in October 2010 (Fig. 6a). This positive deviation from 2.5 suggests an N_2O source with relatively low bulk $\delta^{15}N$-N_2O values, which partially counteracts the isotopic imprint left by N_2O consumption and contributes to the community N_2O isotope signatures measured within the RTZ. Indeed, it has been shown by Freymond et al. (2013) that the South Basin sediments represent a net N_2O source with denitrification being the main N_2O production pathway. In summary, the isotope and isotopomer profiles in the RTZ reflect the overlapping isotopic imprints of N_2O production through NH_2OH oxidation at the oxic–anoxic interface, N_2O production through incomplete denitrification, and N_2O reduction to N_2 below the oxic–anoxic interface and in the deep sediments.

The isotopic signature of N_2O consumption in the Lake Lugano North Basin reflects N_2O production through nitrifier denitrification and N_2O consumption through denitrification

In the northern basin of Lake Lugano, N_2O concentrations were generally much lower (i.e., < 13 nmol L^{-1}) than

in the southern basin and barely exceeded tropospheric equilibrium concentrations (Fig. 5a). Maximum N_2O concentrations were measured at 20 m water depth, where we observed a bulk $\delta^{15}N$–N_2O minimum of ~5‰, indicating in situ N_2O production. Nitrification is indicated by the NO_3^- concentration peak observed at the same depth, suggesting close links between NO_3^- regeneration and N_2O production by nitrifying microorganisms. A relatively low SP of 16‰ at this depth, however, implies that here, in contrast to the South Basin RTZ, nitrifier denitrification is the main N_2O source. Below, in the deeper hypolimnion toward the RTZ, the decreasing N_2O concentrations, in tandem with increasing bulk $\delta^{15}N$- and $\delta^{18}O$-N_2O, as well as an increasing SP (up to ~26‰ in the RTZ) all indicate net N_2O consumption, with the N_2O reduction zone being situated about 15 m below the depth of O_2 disappearance. N_2O production through microaerobic NH_4^+ oxidation or nitrifier denitrification in the RTZ cannot be fully excluded, but seems to be of minor importance in the Lake Lugano North Basin (Wenk et al. 2013). The characteristic relationship between the N_2O concentration and the N_2O delta values between 40 m and 125 m depth (Rayleigh plot; Fig. 6b) yielded apparent N and O isotope enrichment factors of $^{15}\varepsilon \approx 3.2‰$ and $^{18}\varepsilon \approx 8.6‰$, respectively. These isotope effects are comparable to what we observed in the South Basin, but are again low compared to previous estimates from natural environments and culture studies (Fig. 1, Table 1). This observation can partially be explained by the fact that the Rayleigh model tends to underestimate the biological isotope effects (e.g., Lehmann et al. 2003; Wenk et al. 2014a), particularly if substrate consumption is almost complete, the substrate pool is not fully homogenized, and the investigated environment violates the closed-system rule of the Rayleigh approach. The apparent underexpression of the isotope effects associated with N_2O consumption in the water column of the Lake Lugano North Basin is likely the result of almost complete consumption and N_2O diffusion limitation at the reaction site within the RTZ. Here, similarly low apparent isotope effects (N, O, and C, respectively) have been observed for lithotrophic NO_3^- reduction (Wenk et al. 2014a), NH_4^+ oxidation (Wenk et al. 2014a), as well as methane oxidation (Blees et al. 2014b), which have been partly attributed to the near-complete consumption of the substrate in a comparatively narrow reaction zone. Low community isotope fractionation may thus be a general feature intrinsic to the North Basin RTZ, independent of the biogeochemical process. However the ratio of ^{18}O vs. ^{15}N enrichment (i.e., the $^{18}\varepsilon$: $^{15}\varepsilon$ ratio) as well as the SP should not be affected by these aspects that bias Rayleigh-based isotope effect estimates, and should be indicative of the dominant process. More precisely, the latter parameters should provide additional constraints on whether N_2O reduction by denitrifying bacteria alone is responsible for the observed trends in the North Basin water column, or whether the observed N_2O concentration and isotope profiles reflect the net effect of combined N_2O production and consumption by denitrification. The ^{18}O to ^{15}N enrichment ratio for the northern basin was approximately 2.5 between 40 m and 125 m depth (Fig. 6b), consistent with observations made for net N_2O consumption in the Eastern Tropical North Pacific (ETNP) (Yamagishi et al. 2007) and in culture experiments (Ostrom et al. 2007). Whereas denitrification in the ETNP can be assumed to be organotrophic, NO_3^- reduction in the Lake Lugano North Basin is mostly sulfide-dependent (Wenk et al. 2013). Our present study thus suggests that an ^{18}O to ^{15}N enrichment ratio of 2.5 is diagnostic for microbial N_2O reduction, independent of its metabolic mode (organotrophic vs. lithotrophic). This in turn is reaffirming our interpretation of the observed N-to-O isotope trends in the South Basin, where we regarded a positive deviation from this ratio as a signal of N_2O production. Similarly, the $\delta^{15}N$ and $\delta^{18}O$ values at 135 m depth in the North Basin, just below the oxic–anoxic interface, do not match the predicted O-to-N trend (Fig. 5b,c) and may hence be indicative of an in situ N_2O source. However, this is a tentative conclusion as it is based on a single measurement only.

Comparison between the two lake basins

In this study, we have provided isotopic evidence for fundamentally different N_2O production and consumption dynamics in the two Lake Lugano basins. The N_2O isotopic signatures in the RTZ of the Lake Lugano South Basin suggest that here N_2O accumulation is the result of a complex combination of N_2O production through nitrification, N_2O production through incomplete denitrification, and N_2O reduction to N_2, all occurring in close proximity to one another. In the Lake Lugano North Basin N_2O is consumed to completion within the RTZ and simultaneous production through (microaerobic) nitrification is thought to be of minor importance at these depths (Wenk et al. 2013). Hence, the N_2O isotope ratio and isotopomer profiles in the hypolimnion can be viewed as quasi-pure N_2O reduction signatures, probably from sulfide-dependent denitrification.

Our results represent a good test case for the interpretation of N_2O isotope signatures in other freshwater and marine environments. For example, we suggest a robust O to N isotope enrichment ratio of ~2.5 for N_2O consumption by lithotrophic or organotrophic denitrification, independent of the environment. Accordingly, we argue that any significant deviation from this fixed O-to-N isotope enrichment trend is due to N_2O production that is co-occurring in or near the zone of N_2O consumption. Modeling efforts will be needed to verify the sensitivity of the dual isotope approach toward N_2O production. Moreover, our data revealed differential N_2O dynamics in the two lake basins, which provide general insight into the controls on N_2O production vs. consumption. We have shown that the environment in the South Basin, which is comparatively dynamic (e.g., with regard to the redox fluctuations), supports more net N_2O production

than the relatively stable conditions found in the North Basin. We speculate that a rapid increase in denitrification rates or physical disturbance of RTZs can cause a delayed or hindered transformation of N_2O to N_2, fostering N_2O accumulation.

In both lake basins, water column N_2O concentrations above the oxic–anoxic interface were comparatively low. This observation suggests that, independent of the geochemical conditions and the actual N_2O dynamics in the RTZ, most of the internally produced N_2O is eventually consumed before reaching the atmosphere. However, N_2O that accumulates in deep water is likely to escape to the atmosphere during (seasonal or sporadic) mixing events through storage flux (Lehmann et al. 2015). Because such non steady-state water-atmosphere N_2O efflux is difficult to capture during regular sampling campaigns, it is even more important to understand the driving mechanisms behind rapid N_2O accumulation in hypolimnetic water.

References

Alexander, R. B., R. A. Smith, and G. E. Schwarz. 2000. Effect of stream channel size on the delivery of nitrogen to the Gulf of Mexico. Nature **403**: 758–761. doi:10.1038/35001562

Babbin, A. R., D. Bianchi, A. Jayakumar, and B. B. Ward. 2015. Rapid nitrous oxide cycling in the suboxic ocean. Science **348**: 1127–1129. doi:10.1126/science.aaa8380

Barbieri, A., and B. Polli. 1992. Description of Lake Lugano. Aquat. Sci. **54**: 181–183. doi:10.1007/BF00878135

Barford, C. C., J. P. Montoya, M. A. Altabet, and R. Mitchell. 1999. Steady-state nitrogen isotope effects of N_2 and N_2O production in *Paracoccus denitrificans*. Appl. Environmen. Microbiol. **65**: 989–994.

Baumann, B., M. Snozzi, J. R. Van der Meer, and A. J. B. Zehnder. 1997. Development of stable denitrifying cultures during repeated aerobic-anaerobic transient periods. Water Res. **31**: 1947–1954. doi:10.1016/S0043-1354(97)00053-5

Blees, J., and others. 2014a. Bacterial methanotrophs drive the formation of a seasonal anoxic benthic nepheloid layer in an alpine lake. Limnol. Oceanogr. **59**: 1410–1420. doi:10.4319/lo.2014.59.4.1410

Blees, J., and others. 2014b. Micro-aerobic bacterial methane oxidation in the chemocline and anoxic water column of deep south-alpine Lake Lugano (Switzerland). Limnol. Oceanogr. **59**: 311–324. doi:10.4319/lo.2014.59.2.0311

Bonner, F. T., J. Kada, and K. G. Phelan. 1983. Symmetry of the intermediate in the hydroxylamine nitrous-acid reaction. Inorg. Chem. **22**: 1389–1391. doi:10.1021/ic001 51a024

Bonner, F. T., and M. N. Hughes. 1988. The aqueous solution chemistry of nitrogen in low positive oxidation states. Comments Inorg. Chem. **7**: 215–234. doi:10.1080/02603598808072309

Braman, R. S., and S. A. Hendrix. 1989. Nanogram nitrite and nitrate determination in environmental and biological materials by vanadium(III) reduction with chemiluminescence detection. Anal. Chemi. **61**: 2715–2718. doi:10.1021/ac00199a007

Casciotti, K. L., D. M. Sigman, M. Galanter Hastings, J. K. Böhlke, and A. Hilkert. 2002. Measurement of the oxygen isotopic composition of nitrate in seawater and freshwater using the denitrifier method. Anal. Chem. **74**: 4905–4912 doi:10.1021/ac020113w

Diem, T., S. Koch, S. Schwarzenbach, B. Wehrli, and C. J. Schubert. 2012. Greenhouse gas emissions (CO_2, CH_4, and N_2O) from several perialpine and alpine hydropower reservoirs by diffusion and loss in turbines. Aquat. Sci. **74**: 619–635. doi:10.1007/s00027-012-0256-5

Fehling, C., and G. Friedrichs. 2011. Dimerization of HNO in aqueous solution: An interplay of solvation effects, fast acid-base equilibria, and intramolecular hydrogen bonding? J. Am. Chem. Soc. **133**: 17912–17922. doi:10.1021/ja2075949

Frame, C. H., and K. L. Casciotti. 2010. Biogeochemical controls and isotopic signatures of nitrous oxide production by a marine ammonia-oxidizing bacterium. Biogeosciences **7**: 2695–2709. doi:10.5194/bg-7-2695-2010

Freymond, C. V., C. B. Wenk, C. H. Frame, and M. F. Lehmann. 2013. Year-round N_2O production by benthic NO_x reduction in a monomictic south-alpine lake. Biogeosciences **10**: 8373–8383. doi:10.5194/bg-10-8373-2013

Garside, C. 1982. A chemiluminescent technique for the determination of nanomolar concentrations of nitrate and nitrite in seawater. Mar. Chem. **11**: 159–167. doi:10.1016/0304-4203(82)90039-1

Heil, J., B. Wolf, N. Bruggemann, L. Emmenegger, B. Tuzson, H. Vereecken, and J. Mohn. 2014. Site-specific ^{15}N isotopic signatures of abiotically produced N_2O. Geochim. Cosmochim. Acta **139**: 72–82. doi:10.1016/j.gca.2014. 04.037

Holzner, C. P., W. Aeschbach-Hertig, M. Simona, M. Veronesi, D. M. Imboden, and R. Kipfer. 2009. Exceptional mixing events in meromictic Lake Lugano (Switzerland/Italy), studied using environmental tracers. Limnol. Oceanogr. **54**: 1113–1124. doi:10.4319/lo.2009.54.4.1113

Hooper, A. B., and K. R. Terry. 1979. Hydroxylamine oxidoreductase of *Nitrosomonas* production of nitric-oxide from hydroxylamine. Biochim. Biophys. Acta **571**: 12–20. doi:10.1016/0005-2744(79)90220-1

Howarth, R. W., and others. 1996. Regional nitrogen budgets and riverine N and P fluxes for the drainages to the North Atlantic Ocean: Natural and human influences. Biogeochemistry **35**: 75–139. doi:10.1007/BF02179825

Jones, L. C., B. Peters, J. S. Lezama Pacheco, K. L. Casciotti, and S. Fendorf. 2015. Stable isotopes and iron oxide mineral products as markers of chemodenitrification. Environ. Sci. Technol. **49**: 3444–3452. doi:10.1021/es504862x

Koba, K., and others. 2009. Biogeochemistry of nitrous oxide in groundwater in a forested ecosystem elucidated by

nitrous oxide isotopomer measurements. Geochim. Cosmochim. Acta **73**: 3115–3133. doi:10.1016/j.gca.2009.03.022

Koroleff, F. 1976. Determination of ammonia, p. 126–133. *In* K. Grasshoff [ed.], Methods of Seawater Analysis. Verlag Chemie.

Lehmann, M. F., P. Reichert, S. M. Bernasconi, A. Barbieri, and J. A. McKenzie. 2003. Modelling nitrogen and oxygen isotope fractionation during denitrification in a lacustrine redox-transition zone. Geochim. Cosmochim. Acta **67**: 2529–2542. doi:10.1016/S0016-7037(03)00085-1

Lehmann, M. F., S. M. Bernasconi, J. A. McKenzie, A. Barbieri, M. Simona, and M. Veronesi. 2004. Seasonal variation of the $\delta^{13}C$ and $\delta^{15}N$ of particulate and dissolved carbon and nitrogen in Lake Lugano: Constraints on biogeochemical cycling in a eutrophic lake. Limnol. Oceanogr. **49**: 415–429. doi:10.4319/lo.2004.49.2.0415

Lehmann, M. F., and others. 2015. Powering up the "biogeochemical engine": The impact of exceptional ventilation of a deep meromictic lake on the lacustrine redox, nutrient, and methane balances. Front. Earth Sci. **3**: 45. doi:10.3389/feart.2015.00045

Liikanen, A., and P. J. Martikainen. 2003. Effect of ammonium and oxygen on methane and nitrous oxide fluxes across sediment-water interface in a eutrophic lake. Chemosphere **52**: 1287–1293. doi:10.1016/S0045-6535 (03)00224-8

Mariotti, A., J. C. Germon, P. Hubert, P. Kaiser, R. Letolle, A. Tardieux, and P. Tardieux. 1981. Experimental determination of nitrogen kinetic isotope fractionation: Some principles; Illustration for the denitrification and nitrification processes. Plant Soil **62**: 413–430. doi:10.1007/BF02374138

McCrackin, M. L., and J. J. Elser. 2010. Atmospheric nitrogen deposition influences denitrification and nitrous oxide production in lakes. Ecology **91**: 528–539. doi:10.1890/08-2210.1

McIlvin, M. R., and K. L. Casciotti. 2010. Fully automated system for stable isotopic analyses of dissolved nitrous oxide at natural abundance levels. Limnol. Oceanogr.: Methods **8**: 54–66. doi:10.4319/lom.2010.8.54

Mengis, M., R. Gächter, and B. Wehrli. 1996. Nitrous oxide emissions to the atmosphere from an artificially oxygenated lake. Limnol. Oceanogr. **41**: 548–553. doi:10.4319/lo.1996.41.3.0548

Mohn, J., B. Tuzson, A. Manninen, N. Yoshida, S. Toyoda, W. A. Brand, and L. Emmenegger. 2012. Site selective real-time measurements of atmospheric N_2O isotopomers by laser spectroscopy. Atmos. Meas. Tech. **5**: 1601–1609. doi:10.5194/amt-5-1601-2012

Mohn, J., and others. 2014. Interlaboratory assessment of nitrous oxide isotopomer analysis by isotope ratio mass spectrometry and laser spectroscopy: Current status and perspectives. Rapid Commun. Mass Spectrom. **28**: 1995–2007. doi:10.1002/rcm.6982

Mosier, A., C. Kroeze, C. Nevison, O. Oenema, S. Seitzinger, and O. van Cleemput. 1998. Closing the global N_2O budget: Nitrous oxide emissions through the agricultural nitrogen cycle—OECD/IPCC/IEA phase II development of IPCC guidelines for national greenhouse gas inventory methodology. Nutr. Cycling Agroecosyst. **52**: 225–248. doi:10.1023/A:1009740530221

Ostrom, N. E., A. Pitt, R. Sutka, P. H. Ostrom, A. S. Grandy, K. M. Huizinga, and G. P. Robertson. 2007. Isotopologue effects during N_2O reduction in soils and in pure cultures of denitrifiers. J. Geophys. Res.-Biogeosci. **112**: 1–12. doi:10.1029/2006JG000287

Otte, S., N. G. Grobben, L. A. Robertson, M. S. M. Jetten, and J. G. Kuenen. 1996. Nitrous oxide production by *Alcaligenes faecalis* under transient and dynamic aerobic and anaerobic conditions. Appl. Environmen. Microbiol. **62**: 2421–2426.

Popp, B. N., and others. 2002. Nitrogen and oxygen isotopomeric constraints on the origins and sea-to-air flux of N_2O in the oligotrophic subtropical North Pacific gyre. Global Biogeochem. Cycles **16**: 12–1–12-10. doi:10.1029/2001GB001806

Poth, M., and D. D. Focht. 1985. ^{15}N kinetic analysis of N_2O production by *Nitrosomonas europaea*: An examination of nitrifier denitrification. Appl. Environmen. Microbiol. **49**: 1134–1141.

Rakshit, S., C. J. Matocha, and M. S. Coyne. 2008. Nitrite reduction by siderite. Soil Sci. Soc. Am. J. **72**: 1070–1077. doi:10.2136/sssaj2007.0296

Rasmussen, R. A., and M. A. K. Khalil. 1986. Atmospheric trace gases: Trends and distributions over the last decade. Science **232**: 1623–1624. doi:10.1126/science.232.4758.1623

Ravishankara, A. R., J. S. Daniel, and R. W. Portmann. 2009. Nitrous oxide (N_2O): The dominant ozone-depleting substance emitted in the 21st century. Science **326**: 123–125. doi:10.1126/science.1176985

Ryabenko, E., A. Kock, H. W. Bange, M. A. Altabet, and D. W. R. Wallace. 2012. Contrasting biogeochemistry of nitrogen in the Atlantic and Pacific Oxygen Minimum Zones. Biogeosciences **9**: 203–215. doi:10.5194/bg-9-203-2012

Santoro, A. E., C. Buchwald, M. R. McIlvin, and K. L. Casciotti. 2011. Isotopic signature of N_2O produced by marine ammonia-oxidizing archaea. Science **333**: 1282–1285. doi:10.1126/science.1208239

Sasaki, Y., and others. 2011. Biogeochemistry of nitrous oxide in Lake Kizaki, Japan, elucidated by nitrous oxide isotopomer analysis. J. Geophys. Res. **116**: 1–10. doi:10.1029/2010JG001589

Schmidt, H. L., R. A. Werner, N. Yoshida, and R. Well. 2004. Is the isotopic composition of nitrous oxide an indicator for its origin from nitrification or denitrification? A theoretical approach from referred data and microbiological

and enzyme kinetic aspects. Rapid Commun. Mass Spectrome. **18**: 2036–2040. doi:10.1002/rcm.1586

Snider, D. M., S. L. Schiff, and J. Spoelstra. 2009. $^{15}N/^{14}N$ and $^{18}O/^{16}O$ stable isotope ratios of nitrous oxide produced during denitrification in temperate forest soils. Geochim. Cosmochim. Acta **73**: 877–888. doi:10.1016/j.gca.2008.11.004

Snider, D. M., J. J. Venkiteswaran, S. L. Schiff, and J. Spoelstra. 2015. From the ground up: Global nitrous oxide sources are constrained by stable isotope values. PloS One **10**: e0118954. doi:10.1371/journal.pone.0118954

Stein, L. Y., R. Roy, and P. F. Dunfield. 2012. Aerobic methanotrophy and nitrification: Processes and connections. *In* eLS. John Wiley & Sons, Ltd: Chichester. doi:10.1002/9780470015902.a0022213

Stieglmeier, M., M. Mooshammer, B. Kitzler, W. Wanek, S. Zechmeister-Boltenstern, A. Richter, and C. Schleper. 2014. Aerobic nitrous oxide production through N-nitrosating hybrid formation in ammonia-oxidizing archaea. ISME J **8**: 1135–1146. doi:10.1038/ismej.2013.220

Sutka, R. L., N. E. Ostrom, P. H. Ostrom, H. Gandhi, and J. A. Breznak. 2003. Nitrogen isotopomer site preference of N_2O produced by *Nitrosomonas europaea* and *Methylococcus capsulatus* Bath. Rapid Commun. Mass Spectrom. **17**: 738–745. doi:10.1002/rcm.968

Sutka, R. L., N. E. Ostrom, P. H. Ostrom, H. Gandhi, and J. A. Breznak. 2004. Erratum: Nitrogen isotopomer site preference of N_2O produced by *Nitrosomonas europaea* and *Methylococcus capsulatus* Bath. Rapid Commun. Mass Spectrom. **18**: 1411–1412. doi:10.1002/rcm.1482

Sutka, R. L., N. E. Ostrom, P. H. Ostrom, J. A. Breznak, H. Gandhi, A. J. Pitt, and F. Li. 2006. Distinguishing nitrous oxide production from nitrification and denitrification on the basis of isotopomer abundances. Appl. Environ. Microbiol. **72**: 638–644. doi:10.1128/AEM.72.1.638-644.2006

Toyoda, S., and N. Yoshida. 1999. Determination of nitrogen isotopomers of nitrous oxide on a modified isotope ratio mass spectrometer. Anal. Chem. **71**: 4711–4718. doi:10.1021/ac9904563

Toyoda, S., and others. 2002. Production mechanism and global budget of N2O inferred from its isotopomers in the western North Pacific. Geophys. Res. Lett. **29**: 4. doi:10.1029/2001GL014311

Toyoda, S., H. Mutobe, H. Yamagishi, N. Yoshida, and Y. Tanji. 2005. Fractionation of N_2O isotopomers during production by denitrifier. Soil Biol. Biochem. **37**: 1535–1545. doi:10.1016/j.soilbio.2005.01.009

Toyoda, S., H. Iwai, K. Koba, and N. Yoshida. 2009. Isotopomeric analysis of N_2O dissolved in a river in the Tokyo metropolitan area. Rapid Commun. Mass Spectrom. **23**: 809–821. doi:10.1002/rcm.3945

Treusch, A. H., S. Leininger, A. Kletzin, S. C. Schuster, H. P. Klenk, and C. Schleper. 2005. Novel genes for nitrite reductase and Amo-related proteins indicate a role of uncultivated mesophilic crenarchaeota in nitrogen cycling. Environmen. Microbiol. **7**: 1985–1995. doi:10.1111/j.1462-2920.2005.00906.x

Wang, W. C., Y. L. Yung, A. A. Lacis, T. Mo, and J. E. Hansen. 1976. Greenhouse effects due to man-made perturbations of trace gases. Science **194**: 685–690. doi:10.1126/science.194.4266.685

Weiss, R. F., and B. A. Price. 1980. Nitrous-oxide solubility in water and seawater. Mar. Chem. **8**: 347–359. doi:10.1016/0304-4203(80)90024-9

Wenk, C. B., and others. 2013. Anaerobic ammonium oxidation (anammox) bacteria and sulfide-dependent denitrifiers coexist in the water column of a meromictic south-alpine lake. Limnol. Oceanogr. **58**: 1–12. doi:10.4319/lo.2013.58.1.0001

Wenk, C. B., J. Zopfi, J. Blees, M. Veronesi, H. Niemann, and M. F. Lehmann. 2014a. Community N and O isotope fractionation by sulfide-dependent denitrification and anammox in a stratified lacustrine water column. Geochim. Cosmochim. Acta **125**: 551–563. doi:10.1016/j.gca.2013.10.034

Wenk, C. B., J. Zopfi, W. S. Gardner, M. J. McCarthy, H. Niemann, M. Veronesi, and M. F. Lehmann. 2014b. Partitioning between benthic and pelagic nitrate reduction in the Lake Lugano south basin. Limnol. Oceanogr. **59**: 1421–1433. doi:10.4319/lo.2014.59.4.1421

Westley, M. B., H. Yamagishi, B. N. Popp, and N. Yoshida. 2006. Nitrous oxide cycling in the Black Sea inferred from stable isotope and isotopomer distributions. Deep-Sea Res. **53**: 1802–1816. doi:10.1016/j.dsr2.2006.03.012

Wrage, N., G. L. Velthof, M. L. Van Beusichem, and O. Oenema. 2001. Role of nitrifier denitrification in the production of nitrous oxide. Soil Biol. Biochem. **33**: 1723–1732. doi:10.1016/S0038-0717(01)00096-7

Wullstein, L. H., and C. M. Gilmour. 1966. Non-enzymatic formation of nitrogen gas. Nature **210**: 1150–1151. doi:10.1038/2101150a0

Wunderlin, P., M. F. Lehmann, H. Siegrist, B. Tuzson, A. Joss, L. Emmenegger, and J. Mohn. 2013. Isotope signatures of N_2O in a mixed microbial population system: Constraints on N_2O producing pathways in wastewater treatment. Environ. Sci. Technol. **47**: 1339–1348. doi:10.1021/es303174x

Yamagishi, and others. 2007. Role of nitrification and denitrification on the nitrous oxide cycle in the eastern tropical North Pacific and Gulf of California. J. Geophys. Res.-Biogeosci. **112**: 1–15. doi:10.1029/2006JG000227

Yamazaki, T., T. Hozuki, K. Arai, S. Toyoda, K. Koba, T. Fujiwara, and N. Yoshida. 2014. Isotopomeric characterization of nitrous oxide produced by reaction of enzymes extracted from nitrifying and denitrifying bacteria. Biogeosciences **11**: 2679–2689. doi:10.5194/bg-11-2679-2014

Yoh, M., H. Terai, and Y. Saijo. 1983. Accumulation of nitrous-oxide in the oxygen deficient layer of fresh-water lakes. Nature **301**: 327–329. doi:10.1038/301327a0

Yoshida, N. 1988. ^{15}N-depleted N_2O as a product of nitrification. Nature **335**: 528–529. doi:10.1038/335528a0

Zhu, X., M. Burger, T. A. Doane, and W. R. Horwath. 2013. Ammonia oxidation pathways and nitrifier denitrification are significant sources of N_2O and NO under low oxygen availability. Proc. Natl. Acad. Sci. **110**: 6328–6333. doi: 10.1073/pnas.1219993110

Acknowledgments

Mark Rollog, Yuji Sasaki, as well as the late Gijs Nobbe, and the late Marianne Caroni are thanked for their help in the laboratory and Marco Simona and Stefano Beatrizotti for sampling assistance on Lake Lugano. Two anonymous reviewers are thanked for valuable comments on an earlier version of this manuscript. This study was funded through the Swiss National Science Foundation project 129491 (Nitrogen elimination pathways and associated isotope effects in Swiss eutrophic Lake Lugano) granted to MFL and JZ.

Submitted 16 September 2015
Revised 8 March 2016
Accepted 15 April 2016

Associate editor: Maren Voss